

# Zn/Br<sub>2</sub> Cell: Effects of Plated Zinc and Complexing Organic Phase

Egwu E. Kalu and Ralph E. White

Center for Electrochemical Engineering, Dept. of Chemical Engineering, Texas A&M University, College Station, TX 77843

*A model is presented for a zinc/bromine cell that considers the effects of an increase or a decrease in the cathode channel width due to zinc removal on discharge and zinc deposition on charge, respectively. The model also includes the effect of an organic bromine complexing agent (OCA) on the cell performance. Changes in the channel width affect the catholyte velocity, cathode side pressure drop, mass transfer and potential drop in the cell, while the inclusion of the bromine complexing organic phase shows a marked effect on the available bromine in the aqueous phase.*

*It is shown that during discharge, the release of complexed Bromine by the OCA could degrade the cell performance. A simple equation is derived and used to express the relationship between the total bromine in the organic phase and the bromine in the aqueous phase.*

## Introduction

The need by electric utilities to operate at optimum capacity, to satisfy cyclic demands of the customers, to generate power on peak at low cost, and above all to be cost-effective has increased interest in the development of the zinc/bromine (Zn/Br<sub>2</sub>) flow battery. The Zn/Br<sub>2</sub> battery is highly regarded as a candidate for load-leveling (peak-shaving) in the electric utility industry, and is also considered as a possible device for automobile propulsion. The potential advantages offered by the Zn/Br<sub>2</sub> flow battery as a possible load-leveler include the abundance and low cost of the active materials (reactants), high cell voltage, good specific energy, good electrochemical reversibility and ambient temperature operation.

The Zn/Br<sub>2</sub> battery is a complex system whose performance depends on a large number of variables. Mathematical analysis affords a practical means of studying the system variables, constraints and performance. An accurate solution of a comprehensive Zn/Br<sub>2</sub> cell model poses a mathematical challenge. Consequently, simplifying assumptions are used to avoid such a challenge. Such simplifications were used in the previously developed Zn/Br<sub>2</sub> cell model (Evans and White, 1987b).

Modeling of a physical system could be based on a theoretically or empirically derived relations or a combination of the two. A theoretically based model uses fundamental principles and, therefore, could be applied to study a particular

system or related systems of interest, while empirically derived model is often limited to the system from which the relations or correlations describing the model were derived. The models due to Putt (1979), Lee (1981), Lee and Selman (1982a), Mader and White (1986), Evans and White (1987a), Van Zee et al. (1984), and Simpson and White (1990) are based on theory, while the work of Bolsted et al. (1988) couples theoretical foundation with empirically derived results. As a result of the simplifying assumptions used in developing these models, many important physical features of the system were ignored. There is a need, therefore, to present another model in which some of the features not yet accounted for are included and some of the nonpertinent assumptions discarded. The present model aims to fulfill these objectives.

The different mathematical models of the Zn/Br<sub>2</sub> battery, previously developed, were aimed at understanding the system to prescribe optimal design. Evans and White (1987b) reviewed the work performed up to 1987. Since that review, Simpson and White (1990) and Bolsted et al. (1988) have presented some results on the Zn/Br<sub>2</sub> battery. Simpson and White (1990) presented an algebraic model of the Zn/Br<sub>2</sub> cell with and without recirculation. The model is a simplification of the more involved finite-differenced based models of Mader and White (1986) and Evans and White (1987a). They showed that an optimum value of the applied potential (constant voltage charge) exists for the Zn/Br<sub>2</sub> battery and it depends on the feed composition. The model, however, cannot be used to

Correspondence concerning this article should be addressed to R. E. White.

account for the zinc deposition nor for the role of the complexing organic phase.

The model of Bolsted et al. (1988) couples theoretical foundation with empirically-derived results. It is capable of predicting charge and discharge voltages, coulombic, voltaic and energy efficiencies, and effects of design changes on the parameters mentioned above. The model incorporates some of the theoretical basis of the Van Zee et al. (1984) model, and thus accounts for coulombic losses in the cell and for the power used in the operation of the shunt current protection system. The model accounts for the changing cathode gap due to zinc deposition. The resistivity of the anolyte or the catholyte electrolyte and the open circuit voltage of the battery during charge are treated as empirical functions of the state of charge. The fluid flow part of the model is based on more fundamental governing equations, and thus can be applied to any flow battery. The model is limited in that it relies heavily on empirical equations to achieve a good match between results predicted by the model and the results of actual laboratory battery testing. This is a disadvantage, since some pertinent parameters of the models are considered proprietary by the developers. The model cannot predict the conversion per pass. Other useful studies on the development of the Zn/Br<sub>2</sub> battery include those of Tomazic (1989) and Bolsted (1991).

In the present work, material balances for the species in the electrochemical reactor at steady state were set up and the resulting partial differential equations were converted to algebraic equations by the finite difference method. These simultaneous algebraic equations were solved using Newman's (1973) band method. Then, the material balance equations for the recirculating tanks, which were coupled to the electrochemical reactor, were integrated for each time step. The time step for the unsteady-state simulation was obtained by assuming that the total zinc consumed in the system could only have been through electrochemical reaction. Thus, by knowing the amount of zinc converted at each steady-state run, an estimate of the time required for the unsteady-state calculation was obtained.

The change in the geometry of the cell that resulted from the plated or removed zinc and its effects on cell performance were included. The role of the bromine complexing agent, otherwise called organic complexing agent (OCA), on the performance of the cell was also included. The model is able to predict the conversion per pass and the time dependence of the system. The present work draws from the works of Evans and White (1987a) and Mader and White (1986); however, the inclusion of the variable channel width, the pressure changes, convective flow across the separator, bromine complexation and conversion per pass are unique to the present model.

The present model shows that:

1. Ignoring the changes in the channel leads to predictions that differ from those obtained when the effects are considered. For very short times, these differences are not significant, but may become significant when the cell is operated for longer times.
2. On the inclusion of the organic complexing agent, the model predicts an improved cell performance during charge.
3. The recirculation of the OCA improves mixing and leads to more bromine removal from the system during charge. This and the use of large volumes of OCA improve the predicted total cell efficiency.
4. It is shown that the OCA can be characterized based

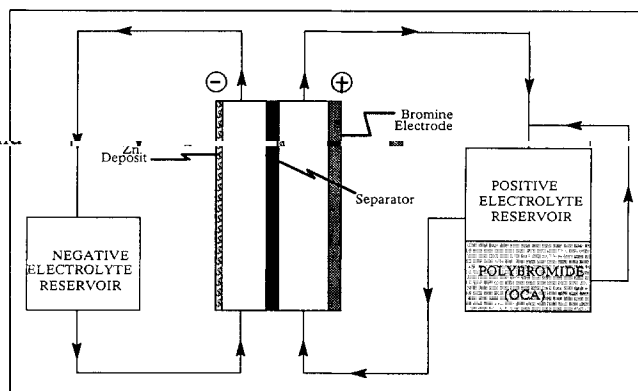
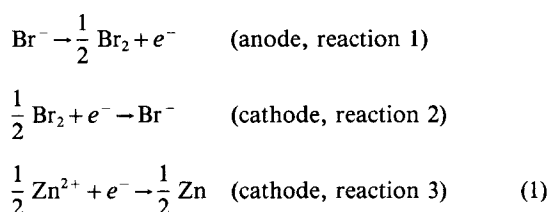


Figure 1. Zn/Br<sub>2</sub> cell with associated flow system (charge mode).

on the coefficient and exponent of an equation expressing the relationship between the total bromine in the organic phase and the bromine in the aqueous phase.

5. The model showed that the consideration of both the organic phase and plated or removed zinc was needed in making relevant predictions of design value.

The zinc/bromine flow battery is being developed by a number of companies with some design differences. Some of the different cell designs, including the so-called Exxon and Gould designs, are described by Chamberlin (1983). However, a typical zinc/bromine flow battery consists of stacks of individual electrochemical cells, each containing two electrodes at which reversible reactions occur as shown in Eq. 1. During the charging of a zinc/bromine battery, an aqueous solution of zinc bromide containing other materials is recirculated in two different streams: one at the anode side and the other at the cathode. A typical cell arrangement is as shown in Figure 1.



Complexation of Br<sup>-</sup> and Br<sub>2</sub> to form tribromide ions (Br<sub>3</sub><sup>-</sup>), Br<sub>2</sub> and Br<sub>3</sub><sup>-</sup> to form pentabromide ions (Br<sub>5</sub><sup>-</sup>), and zinc ions reacting with bromide to form several different zinc/bromine complexes occurs in the bulk of the electrolytic solution. The pentabromide ions and the zinc bromide complexes are not included in this model. During discharge, the reverse electrochemical reactions occur when the battery is connected to a load. The complexed bromine in the organic phase is then released to the aqueous phase.

## The Model Equations

Most of the assumptions made by Mader and White (1986) and Evans and White (1987a) on the electrochemical reactor (ECR) are applicable, except for the separator region in which convective flow is allowed. The organic complexing agent does not enter into the electrochemical reactor: one-phase flow is assumed within the ECR, thus limiting the OCA to the anode recirculating tank. It is also assumed that there is no pressure gradient across the flow channel region. The pressure drop in

the flow channel is in the direction of electrolyte flow and decreases linearly. For the electrochemical reactor, we will present only the modified species material balance equation in the separator. The equations relating to the recirculating tanks, bromine complexation, and time stepping technique are also presented.

The governing equations for the flow channels, separator, and porous electrode are the species material balance equations and the electroneutrality conditions. The steady-state equations used are as presented by Mader and White (1986) and Evans and White (1987a) except for the governing equations in the separator region. The governing equation pertaining to the separator have a flow term normal to the separator (Van Zee et al., 1986). The governing equation for species  $i$  in the interior of the separator is given by:

$$-\nabla \cdot N_i + R_i = 0 \quad (2)$$

where

$$N_i = -\frac{D_i}{N_m} \nabla c_i - z_i \frac{D_i}{N_m} F c_i \nabla \Phi + v_s c_i \quad (3)$$

$N_m$  is the MacMullin's number, defined as the ratio of the tortuosity of the separator (diaphragm) to its porosity (Van Zee, 1984). The superficial velocity,  $v_s$  and the MacMullin's number  $N_m$  can be related to the velocity  $v$  inside the pores by:

$$v = \frac{v_s}{\frac{\tau}{\epsilon} N_m} \quad (4)$$

To account for the superficial electrolyte velocity  $v_s$  through the separator, knowledge of the pressure drop across the separator is required. An approximate relation for the pressure drop per unit length in a horizontal channel is estimated from Hansen (1967) as:

$$\frac{\Delta p}{\Delta L} = \frac{12\mu v_{avg}}{h^2} \quad (5)$$

where the lefthand side is the pressure drop per unit length. For the convective flow velocity in the separator, Darcy's law is used where

$$v_s = -\frac{\beta dp}{\mu dy} \approx -\left(\frac{\beta}{\mu}\right) \left(\frac{\Delta p}{\Delta y}\right) \quad (6)$$

Here,  $\Delta y$  refers to the thickness of the separator,  $\beta$  is the permeability of the separator material, and  $\mu$  is the viscosity of the electrolyte solution within the separator. Since the one-step method of Mader and White (1986) was used, the pressure drop per unit length of the reactor (assuming linearly decreasing pressure in each of the two compartments of the flow cell) could be calculated. If the pressure drop per unit length of the reactor on the anode and cathode sides are represented as  $P_{LA}$  and  $P_{LC}$ , respectively, then the flux for species  $i$  in the interior of the separator is given by:

$$N_i = -D_{i,e} \nabla c_i - z_i \frac{D_{i,e}}{RT} F c_i \nabla \Phi - \frac{\beta}{\mu S_p} (P_{LA} - P_{LC}) c_i \quad (7)$$

where  $D_{i,e}$  is the effective diffusion coefficient of species  $i$  in the separator. For the solution of the equations, second-order upwind differencing technique (Vanka, 1987) was used for the separator interior.

The material balance equation for the reservoir tank and the electroneutrality condition are the governing equations for the tank. Assuming that the reservoir behaves as a continuous stir tank reactor (CSTR), the unsteady-state mass balance equation for each tank is given as follows (Holland and Anthony, 1979):

$$\frac{dc_{i,feed}}{dt} = \frac{q}{V_{Tr}} [c_{i,avg}(t, x=L) - c_{i,feed}(t)] + R_{cstr,i} \quad (8)$$

where

$V_{Tr}$  = volume of the recirculation tank (constant volume)

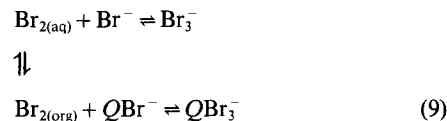
$q$  = volumetric flow rate through the system

$c_{i,feed}(t)$  = inlet concentration of species  $i$  to the electrochemical reactor and outlet concentration of the recirculation tank

$c_{i,avg}(t, x=L)$  = outlet concentration of species  $i$  from the electrochemical reactor, but inlet concentration into the recirculation tank

$R_{cstr,i}$  = production rate of  $i$  in the recirculation tank

The reactions of interest in the anode recirculation tank are given by:



where  $Q\text{Br}^-$  can be any quaternary ammonium bromide capable of acting as the bromine complexing agent. The following equilibrium ratios are expressed for the reactions of Eq. 9:

Between the organic phase and the aqueous phase we have:

$$K_D = \frac{[\text{Br}_{2(org)}]}{[\text{Br}_{2(aq)}]} \quad (10)$$

In the aqueous phase, the equilibrium condition for the species is given by:

$$K_f = \frac{[\text{Br}_3^-]}{[\text{Br}^-][\text{Br}_{2(aq)}]} \quad (11)$$

while for the complexing organic phase, the equilibrium constant  $K_o$  is:

$$K_o = \frac{[Q\text{Br}_3^-]}{[\text{Br}_{2(org)}][Q\text{Br}^-]} \quad (12)$$

Hence, the equilibrium ratio for the total bromine in the organic phase to the total bromine in aqueous phase can be expressed as:

$$D = \frac{[\text{Br}_{2(org)}] + [Q\text{Br}_3^-]}{[\text{Br}_{2(aq)}] + [\text{Br}_3^-]} \quad (13)$$

Using Eqs. 11 and 12 for  $[\text{Br}_3^-]$  and  $[Q\text{Br}_3^-]$ , respectively, and substituting into Eq. 13, we obtain on simplification

$$D = \frac{K_D(1 + K_o[Q\text{Br}^-])}{1 + K_f[\text{Br}^-]} \quad (14)$$

Values of  $D$  have been determined (Eustace, 1980; Kinoshita et al., 1982) for some  $QBr^-$  systems although these were erroneously referred to as the distribution coefficient. The distribution coefficient is  $K_D$ , which is a thermodynamic equilibrium constant. Only  $D$  (the distribution ratio), not  $K_D$  (the distribution constant or coefficient), can be determined experimentally by the analysis of the two-phase system. This is because, at equilibrium, the bromine exists as a mixture of chemical forms in both phases. Mader and White (1986) and Evans and White (1987a) included in their cell models the aqueous-phase equilibrium reaction involving  $Br_2$ ,  $Br^-$ , and  $Br_3^-$ . The value of the equilibrium constant  $K_f$  for Eq. 11 is  $17,000 \text{ cm}^3/\text{mol}$ .

For simplicity, let us assume that the concentration of  $QBr^-$  is very large. At large concentration of  $QBr^-$ ,  $K_o$  will be negligible and thus Eq. 14 reduces to:

$$D = \frac{K_D}{1 + K_f[Br^-]} \quad (15)$$

Using the data of Kinoshita et al. (1982), with the concentrations expressed in  $\text{mol}/\text{cm}^3$ , a correlation for  $D$  can be obtained:

$$D = 0.0703([c_{Br_2(aq)}] + [c_{Br_3^-}])^{-0.785} \quad (16)$$

and for a correlation of total aqueous-phase bromine concentration against the total bromine in the organic phase, we obtain:

$$[c_{Br_2(org)}]_T = 0.108[c_{Br_2(aq)}]_T^{0.2609} \quad (17)$$

where the use of subscript  $T$  represents the total available bromine in the given phase. For instance, in the aqueous phase, the total bromine includes the uncomplexed  $Br_2$  and the bromine that will be released from the tribromide ion when a titrating agent such as iodide is added. The coefficient and the exponent on the righthand side of Eq. 17 are assumed to depend on the characteristics of a given organic complexing agent. Thus, the use of a number other than 0.2609 for the exponent or 0.108 for the coefficient of the above equation is equivalent to the use of an OCA whose properties differ from the one reported by Kinoshita et al. (1982).

The relationship between the circulating tanks and the ECR was used to obtain an estimate of the time required for a steady-state pass of reactants through the electrochemical reactor. The material balance for the storage tank (Eq. 8) is coupled to that of the ECR. A material balance over half of the cell, for instance, the cathode side, can be related to the storage tank as follows:

$$q(c_{i,feed} - c_{i,avg}) = \frac{wL \langle i_{avg} \rangle}{zF} + wL \langle N_{i,sep} \rangle + V_{cell} R \quad (18)$$

where  $\langle N_{i,sep} \rangle$  is the average flux of species  $i$  across the separator. Substituting the above into Eq. 8, we obtain:

$$V_{Tr} \frac{dc_{i,feed}}{dt} = \frac{wL \langle i_{avg} \rangle}{zF} + wL \langle N_{i,sep} \rangle + R_i V_{cell} + V_{Tr} R_{cstr,i} \quad (19)$$

If we consider a species  $i$ , which is not involved in any homogeneous reaction within the reactor nor the recirculating tank, then the  $R$  terms in the above equation can be eliminated and the equation integrated. An example of such a species in the present model is the zinc ion. Thus, integrating the reduced equation from  $t = t_1$  to  $t = t_2$  and simplifying, we obtain:

$$c_i^p = 1.0 + \frac{(t_2 - t_1)}{c_i^{t_1} V_{Tr}} \left[ \frac{wL \langle i_{avg} \rangle}{zF} + \langle N_{i,sep} \rangle wL \right] \quad (20)$$

where  $c_i^p$  is the fractional change of the concentration of  $i$  over the time period  $(t_2 - t_1)$ .

## Boundary and Initial Conditions

The boundary conditions for the electrochemical reactor model were taken at:

1. The deposit surface (on the zinc electrode)
2. The porous (Bromine) electrode backing (current collector)
3. The separator/electrolyte interface
4. Porous electrode/electrolyte boundary
5. The reactor entrance.

For the zinc deposit/electrolyte interface, the flux of each ionic species  $i$  is equal to the sum of its reaction rate at the interface. The boundary condition used by Mader and White (1986) is applicable here. The continuity of flux of each species is used to account for the boundary conditions for cases 3 and 4 as in Evans and White (1987a). For the separator/electrolyte interface, however, the presence of the diffusion term in the separator-governing equation means that an upwind differencing scheme (Vanka, 1987) must be adopted for stability. Here, the sign of the convective coefficient determines the differencing scheme to be adopted. It must be noted that there is a pressure variation within the separator. The variation in the pressure drop (within the separator) is such that the side of the separator nearest to a channel gap must have an equal pressure to that channel gap. (No variation in pressure is assumed across the channel gaps.) At the backing plate, the flux of each species is zero and thus,

$$N_{ni} = 0 \quad (21)$$

This boundary condition was used in the work of Evans and White (1987a). The electroneutrality condition must be satisfied at all the boundaries. The initial conditions are the feed condition for the species, while the potential drop  $\Phi$  does not require an initial condition.

## Parameters

The fixed parameter values used for the  $ZnBr_2$  cell model are given in Table 1. Except for the bromine exchange current density,  $i_{Oj,ref}$ , the parameters used by Evans and White (1987a) were used in the present model. The input variables to the model include: the width  $w$  and length of the electrode  $L$ , the volumetric flow rate of the electrolytes,  $q_a$  and  $q_c$ ; the flow channel width  $h$ ; the MacMullin number and permeability of the separator material,  $N_m$  and  $\beta$ ; the thickness of the separator  $S_s$ ; the MacMullin number and the thickness of the porous electrode,  $N_{m,PE}$  and  $S_{PE}$ ; the specific active surface area  $a$  of

**Table 1. Fixed Parameter Values for the Zn/Br<sub>2</sub> Cell**

Kinetic and Thermodynamic ( $T=298.15\text{ K}$ )						
Reaction $j$	$i_{0j,\text{ref}}^*$ $\text{A}/\text{cm}^2 \times 10^4$	$\alpha_{aj}$	$\alpha_{cj}$	$n_j$	$U_j^\theta$ V	$U_{j,\text{ref}}$ V
1	1.861	0.5	0.5	1	1.087	1.80928
2	1.861	0.5	0.5	1	1.087	1.80928
3	8,409	0.5	0.5	1	-0.763	-0.008904

**Stoichiometry and Electrochemical Reaction Orders**

Species $i$	Eqs. 1 and 2 ( $j=1,2$ )			Eq. 3 ( $j=3$ )		
	$S_{ij}$	$P_{ij}$	$Q_{ij}$	$S_{ij}$	$P_{ij}$	$Q_{ij}$
Na <sup>+</sup>	0	0	0	0	0	0
Br <sup>-</sup>	1	1	0	0	0	0
Br <sub>2</sub>	-1/2	0	1/2	0	0	0
Zn <sup>2+</sup>	0	0	0	-1/2	0	1/2
Br <sub>3</sub> <sup>-</sup>	0	0	0	0	0	0
QBr <sup>-</sup>	0	0	0	0	0	0

**Transport and Reference Concentrations**

Species $i$	$z_i$	$D_i$ $\text{cm}^2/\text{s} \times 10^5$	$c_{i,\text{ref}}$ $\text{mol}/\text{cm}^3 \times 10^3$	$\theta_{i,\text{feed}}^{**}$
Na <sup>+</sup>	1	1.334	1.0	1.0
Br <sup>-</sup>	-1	2.3084	1.08	2.7306
Br <sub>2</sub>	0	1.310	0.05	0.0203
Zn <sup>2+</sup>	2	0.754	0.5	2.0
Br <sub>3</sub> <sup>-</sup>	-1	1.310	0.92	0.0554
QBr <sup>-</sup>	-1	—	8.0	1.029619

\*The parameters are from Evans and White (1987a) except for the exchange current densities of reactions 1 and 2 of Mader and White (1986). They are chosen not to replicate the common operating range of the Zn/Br<sub>2</sub> cell, but to illustrate the effects of various parameters on the model results.

\*\*Initial charging feed compositions are the same for each channel. For initial discharge, the feed to each channel was the outlet composition after a certain charging period.

the porous electrode, either the applied cell potential ( $E_{\text{cell}} = U_{PE} - U_c$ ) on charge or ( $E_{\text{cell}} = U_{PE} - U_d$ ) on discharge or the cell current density  $i_n$ ; the recirculation tank volume,  $V_{a,T_r}$  and  $V_{c,T_r}$ ; the organic complexing agent flow rate  $q_o$  and total volume  $V_{o,T_r}$ ; and the nature or type of OCA characterized by the exponent and coefficient of Eq. 17. For the present work, most of the parameters were fixed except for the electrolyte and OCA flow rates, the flow channel width and the current. The electrolyte flows were varied between 2.496 to 7.8 cm<sup>3</sup>/s, the OCA rate studied was for 0 and 2.0 cm<sup>3</sup>/s, and its volume effect study was for 500 and 1,000 cm<sup>3</sup>. For constant current discharge, the current densities were varied between 10.0 and 15.0 mA/cm<sup>2</sup>. To obtain the density  $\rho$  and viscosity  $\mu$  of the electrolytes, correlations reported by Lee and Selman (1982b) were used. These correlations depend on temperature and ZnBr<sub>2</sub> concentration. The resulting expressions are given in Table 2.

## Solution Approach

The steady-state material balance equation and the appropriate boundary condition for each region of the cell was solved using the one-step method as outlined by Mader and White (1986). The Newman's band method (1973) for calculating concentration and potential distributions was used. The average exit concentration of species  $i$  from the cell was taken as the concentration from the cell at time  $t_1$ . To update the concentration of  $i$  in the recirculating tank at time  $t_2$ , where

**Table 2. Physical Model Parameters**

$\rho^*$	$1.0405 \times 10^{-2} + 0.171c_{\text{Zn}^{2+}} - 10.844c_{\text{Zn}^{2+}}^2$
$\mu$	$9.849 \times 10^{-2} + 1.6054c_{\text{Zn}^{2+}} - 248.0c_{\text{Zn}^{2+}}^2$
$\beta^{**}$	$5.0 \times 10^{-13} \text{ cm}^2$
Density of Zinc Deposit	$7.14 \text{ g}/\text{cm}^3$

\*Correlated from Lee and Selman (1982b).

\*\*The permeability was estimated.

$t_2 > t_1$ , Eq. 20 was used. To obtain the appropriate time interval ( $t_2 - t_1$ ) for the update, the constraint

$$c_i^p \leq \psi \quad (22)$$

was used. Here,  $\psi$  is a number chosen such that the quasisteady-state assumption was met. If  $\psi$  is too small, the assumption of steady state was violated, while a large  $\psi$  value closer to 1.0 will lead to an expensive computation time in following the charge/discharge history of the cell. Experience showed that the  $\psi$  values of 0.97–0.99 (for the charge mode) and of 1.03–1.01 (discharge mode) were reliable on the Cray-YMP supercomputer. The  $\langle N_{i,\text{sep}} \rangle$  was evaluated using the concentration distribution within the reactor during the time  $t_1$ . Further,  $i_{\text{avg}}$  was the average current density during the same period.

Theoretically, any species could be used to obtain the time step ( $t_2 - t_1$ ); however, the Zn<sup>2+</sup> species was used here. The use of Zn<sup>2+</sup> was appealing because it was assumed not to be involved in any homogeneous reactions within the system. The calculation adopted here was based on the assumption that the reaction within the ECR was fast and that steady state was achieved instantaneously. The time step ( $t_2 - t_1$ ) was obtained by making the inequality constraint (Eq. 22), one of equality:

$$(t_2 - t_1) = \frac{c_i^1 V_{T_r} [c_i^p - 1.0]}{wL \left[ \frac{\langle i_{\text{avg}} \rangle}{zF} + \langle N_{i,\text{sep}} \rangle \right]} \quad (23)$$

Using the time step above, DASSL (Schiesser, 1988) was used to predict the feed composition by solving a mixture of differential (from material balance over the feed tank, Eq. 8) and algebraic (from the equilibrium conditions, Eqs. 10–17) equations. Once the feed compositions at the end of the time step were determined, the one-step method was used to determine a new steady state. This process was repeated until the desired final operating condition was achieved.

## Results and Discussion

Mader and White (1986) used the total cell energy efficiency as a performance criterion for the Zn/Br<sub>2</sub> cell on charge. The same performance criterion was adopted in this study. The inclusion of recirculating tanks, however, provided more independent variables for study. The performance of the cell under different operating conditions (OCA, volume of the recirculating tanks, electrolyte volumetric flows) and model assumptions (for example, deposition) was studied. The cell performance was studied under (i) constant voltage charge and discharge and (ii) a constant current discharge. In the literature, a battery energy efficiency is quoted often as a single value independent of time. To calculate or evaluate such, often an average value of the cell voltage is used. In this work, however,

the energy efficiencies are reported at different times. Thus, a single energy efficiency can be obtained (for the present work) by taking the average value of the different energy efficiencies obtained at different discharge or charge levels.

### Model Predictions at Various States of Charge

Except when otherwise stated, most of the charging operations were for very low charges (< 25.0% of full charge, where 70% of zinc deposit was considered a full charge). This was also the case for most of the reported constant current discharges.

The exchange current density  $i_{o,j,ref}$  and reference potential  $U_{j,ref}$  were fixed at the values reported in Table 1. This was necessary because the reference concentration was held fixed throughout all states of charge or discharge. The quasisteady-state assumption used in this work was justified because of the low conversion per pass associated with the Zn/Br<sub>2</sub> battery. Further, the one-dimensional assumption was an approximation and was used only as a means of providing a direction in the system design criteria, rather than as an absolute design criteria in itself. Mader and White (1986) compared the accuracy obtained by the one-dimensional model to the complete two-dimensional model. It was shown that the agreement between the two approaches was good enough, if low conversion per pass was the case and the one-dimensional model could be useful for engineering design purposes. Although in the present work the two-dimensional results were not obtained, the material balance closure accounted for over 98.0% of the materials on the inclusion of OCA and zinc deposit in the model. Thus, the inclusion of OCA and zinc deposit was not expected to reduce the accuracy of the one-dimensional approach to anything less than 95.0%. The use of the complete two-dimensional model could reveal the exact relevance and the role of the plated or removed zinc in the performance of the system. This is especially true when the current distribution (important in the formation of dendrites) is considered, that is relaxing the constant current density assumption made in the present model.

Figure 2 shows the effect of organic complexing agent and plated zinc on the predicted cell energy efficiency during a constant voltage charge. The energy efficiency of the cell (or cell efficiency) is defined as the product of the coulombic efficiency and the voltaic efficiency. In the absence of OCA, the model predicted a lower cell efficiency above 45 minutes into the charging operation. This was expected since OCA decreases the available Br<sub>2</sub> (source of cell inefficiency) in the system. During the early period of the charging operation, the available Br<sub>2</sub> concentration was low. Similarly, the bromine distribution within the electrochemical reactor was expected to be low. Thus, the predicted cell performance was the same both in the absence and presence of OCA early in the charging period. However, the predicted cell performance in the absence and presence of OCA differed from each other beyond the 45-minute mark into the discharge process.

The noninclusion of the plated or removed zinc in the model yielded results that differed slightly from the results obtained when the thickness of plated zinc was included. The plating of zinc on the zinc electrode during charge decreases the channel width and makes the zinc electrode potential more negative. When the cathode channel width decreases, the catholyte flow tends to become more turbulent. This increased hydrodynamic

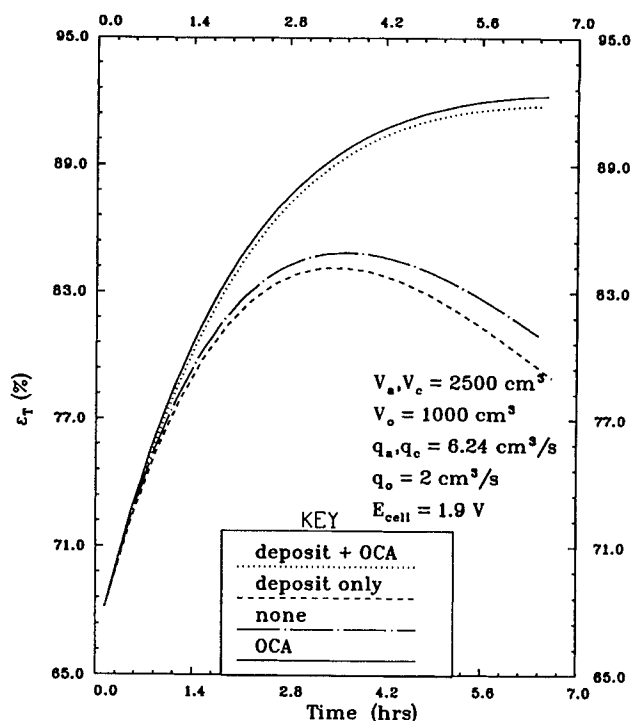
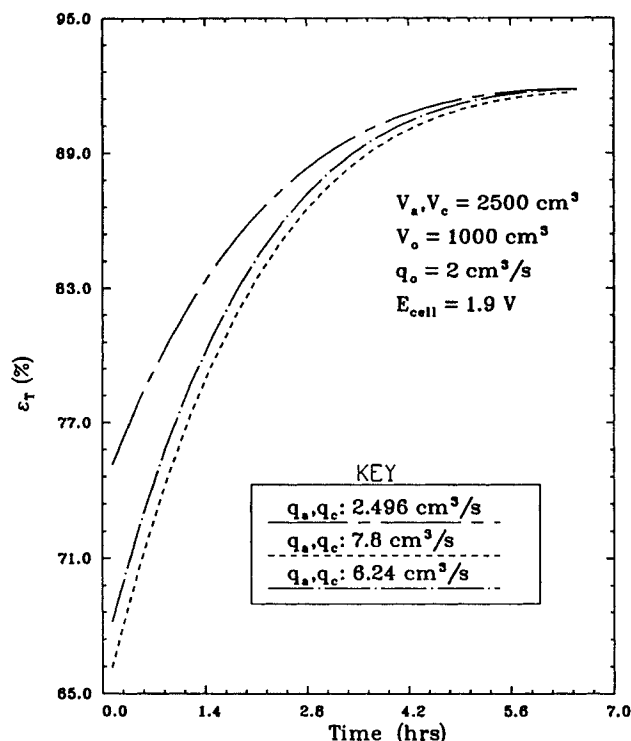


Figure 2. Predicted total cell energy efficiency during constant voltage charge.

activity leads to an increased mixing and concentration redistribution. Although the decrease in channel width favors the voltaic efficiency through the reduction of the IR drop, Figure 2 suggests that this gain in total efficiency was not as significant as the loss in coulombic efficiency due to the increased hydrodynamic activities. Therefore, as Figure 2 shows, there is a need to include the effects of both the OCA and the zinc deposit in the model predictions. The performance trend observed in the absence of OCA and zinc deposit is similar to that obtained by Evans and White (1987a). In comparison with the results of Evans and White (1987a), the inclusion of the recirculating system predicted cell efficiencies of the same order of magnitude under the same operating conditions.

The performance of the cell depended on the electrolyte recirculation rate (Figure 3). In the presence of OCA and with the variable channel width assumption, the model predicted a higher cell efficiency for equal catholyte and anolyte flows ( $q_c$  and  $q_a$ ) of 2.496 cm<sup>3</sup>/s compared to flows of 6.24 or 7.8 cm<sup>3</sup>/s. As the depth of charge increased (up to 4.5 h into the charging operation), the efficiencies of the three flow rates were closer to one another. This behavior could be explained to be due to the hydrodynamic effects in the cell performance. At higher flows, convection favored the movement of the species from the zinc electrode chamber to the bromine electrode chamber. All the species were affected by this convection, including bromine and the zinc ions. The decrease in performance observed at the high electrolyte flow suggests that the zinc ion loss to the bromine electrode chamber, due to convection-induced mass transport, must outweigh the loss of bromine from the zinc electrode chamber due to the same process. Further, high flow rate favors good mixing and brings more bromine into the diffusion layer or nearer the electrode to compete for electrochemical reactions. Such a bromine reduction on the zinc electrode decreases the cell performance.



**Figure 3. Dependence of cell total energy efficiency on electrolyte recirculation rate during constant voltage charge.**

The role of OCA and the plated zinc thickness on the anolyte tank  $\text{Br}_2$  concentration during charge is shown in Figure 4. The inclusion of the plated zinc in the model made a little difference in the predicted results for charging periods less than 2.5 h into the charging process. However, at the end of 2.5 h, the differences between the model predictions for an assumed zinc deposit and lack of deposit increased. The prediction, in which the deposited zinc was considered, was slightly lower than the other case. The difference was more pronounced in the absence of OCA. The bromine concentration in the tank increased in time since it was generated during the charging process.

The percentages of the initial zinc content deposited for the same length of time during constant voltage charge are illustrated in Table 3. The amount of zinc deposited was calculated based on the total zinc available in the system (both anolyte and catholyte contents) at the start of the charging operation. The results in Table 3 suggests that the use of OCA increased the rate of zinc utilization. Table 3 shows that when the changes in the zinc electrode channel width due to zinc deposition were not included, performance prediction obtained was above the value obtained on the inclusion of plated zinc thickness. The difference may be up to 6%. A two-dimensional model may be used to verify this prediction. The model predictions presented here were not meant to be representative of actual cells since some of the parameters were chosen to exemplify the computational method used.

The above results indicate that ignoring the effect of the zinc deposit on Zn/ $\text{Br}_2$  cell model might result in predictions that differ from the actual cell performance values. In engineering design, this deviation might be tolerable. The results

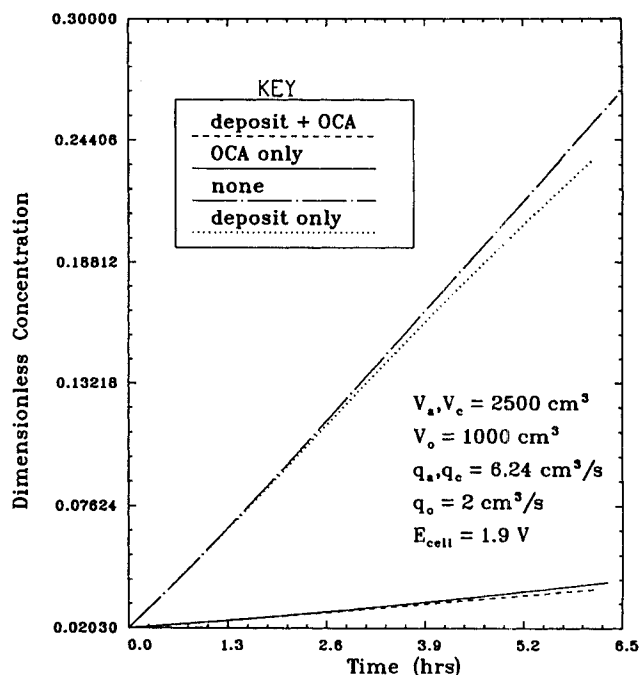


**Figure 4. Anolyte tank bromine concentration during constant voltage charge.**

suggest further that the optimal performance would be obtained if the catholyte and anolyte were recirculated at very low rates. However, the effect of the recirculation rates on other parameters of interest to cell designers was not considered.

## Discharge Mode

Discharges at both constant cell potential and constant current were studied. To simulate a discharge, the feed concentration obtained at the end of a charge mode under a specified model assumption was used. If this was not the case, then it would be possible, for instance, to simulate a discharge in the absence of OCA using an initial feed concentration obtained during a charge process in which OCA was assumed present. Such predictions would be misleading since the available bromine would differ from its actual value at the particular model assumption.

Figure 5 presents the total cell energy efficiency during discharge at a constant cell potential. The cell efficiency decreased with the depth of discharge. Compared to its absence, the presence of OCA led to an improved cell efficiency. This could be explained to be due to the higher  $\text{Br}_2$  concentration that was obtained in the absence of OCA. With a high  $\text{Br}_2$  concentration in the system, more bromine transport across the

**Table 3. Model Predictions at Different Conditions**

Assumption	% Charge Level 6.5 h	% DOD at Constant Voltage 1.9 V, 5.5 h	% DOD at Constant Current 15 mA/cm <sup>2</sup> , 1.4 h
OCA + Deposit	16.5	33.2	36.8
OCA Only	23.0	5.4	21.4
Deposit Only	14.6	72.6	48.0
None	20.5	40.0	27.9

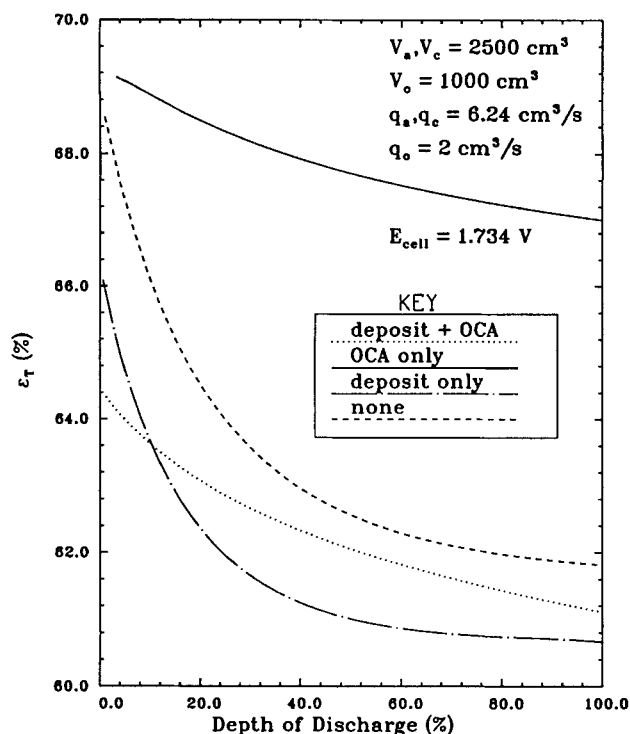


Figure 5. Cell performance during constant voltage discharge.

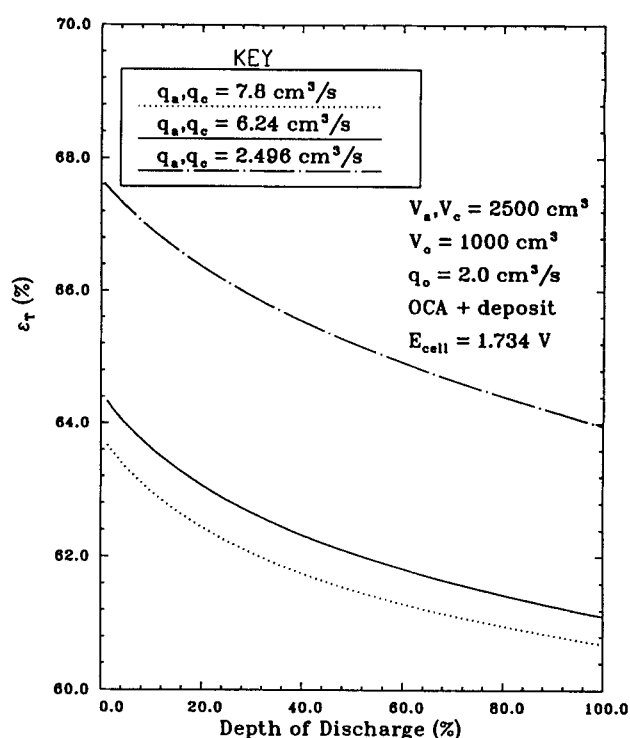


Figure 6. Dependence of cell total energy efficiency on electrolyte recirculation rate during constant voltage discharge.

separator into the zinc electrode chamber occurred. A large amount of bromine favored an increased competition for reaction at the zinc electrode between zinc and bromine. OCA complexes bromine and is capable of releasing the complexed bromine when needed. The control release of bromine by OCA meant a lower bromine current density (the rate of electrochemical reaction of bromine is proportional to its concentration) which was favorable to a higher cell efficiency. The difference between the predicted cell efficiency in the absence of OCA and the value predicted in the presence of OCA increased very slightly with depth of discharge until it approached a constant value. The predicted performance showed that the model in which no deposit was considered was consistently above the predictions in which the deposit thickness was included. In the presence of OCA, the predicted efficiency results showed that the noninclusion of zinc deposition could lead to results of about 5% above the values obtained in the presence of OCA. The differences in these results show the effect of hydrodynamics on both the current and the voltaic efficiencies. The observed behavior was a result of differences in the demand of available bromine in the system occasioned by the channel width and pressure differences.

At a constant voltage, it is observed in Table 3 that for the same discharge period, the depth of discharge (DOD) of the cell was higher in the absence of OCA (72.0%) than in its presence (33.2%). The DOD was calculated based on the change in the amount of zinc in both the anolyte and catholyte tanks. The presence of OCA in the electrolyte inhibited the removal of plated zinc, but favored its plating. When the thickness of the plated zinc was not considered, the model predicted a very low depth of discharge, 5.5% in over five hours of discharge.

The electrolyte flow rate effect on the cell performance is an important parameter for cell development. In Figure 6, a

comparison is made between the cell performance at three different flow rates during a constant voltage discharge. Similar to the predictions made at constant voltage charge, the cell performance increased as the flow rate decreased. However, unlike the charge process, the performance decreased at higher depth of discharges at all flow rates. This could be due to the fact that an increase in channel width with the depth of discharge favored more bromine transport into the zinc electrode chamber for competitive reaction at the zinc electrode. The performance of the cell at constant current discharge showed that the cell performance was favored at higher flow rates. At a constant current, the rate of an electrochemical reaction remains constant, but could be influenced by the rate of mass transfer to the electrode. Higher flow rates favor higher mass transfer.

The predictions in Figure 7 underlies the importance of the inclusion of the organic phase in the cell model. In the absence of the organic phase, the predicted cell energy efficiency falls off for some time, and then rises before a dramatic drop. On the other hand, the presence of the OCA predicted an energy efficiency that decreased very gradually with the depth of discharge before falling off dramatically toward the end of discharge. The noninclusion of the effects of deposited zinc in the model yielded results slightly above what was obtained when it was not considered (OCA present).

The predicted voltaic performance in the cell at constant current discharge is shown in Figure 8. The cell potential dropped linearly with the depth of discharge before a dramatic drop-off toward the end of discharge. The difference between the deposit and nondeposit assumptions remained constant during the duration of the discharge process. The case in which



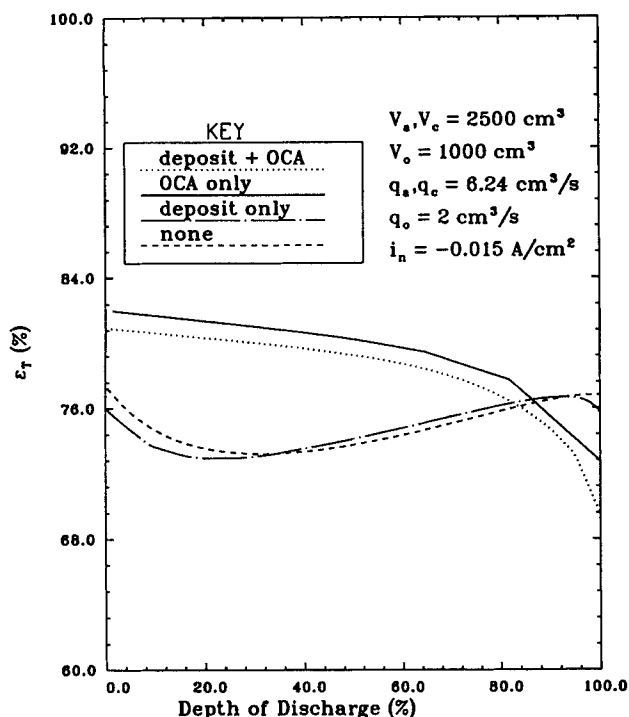


Figure 7. Predicted total cell energy efficiency during constant current discharge.

plated zinc thickness was accounted for yielded the greater voltaic performance. At a constant current, a DOD of nearly 40% was achieved in the presence of OCA in 1.4 h (Table 3). This value was below the same DOD achieved in the absence of OCA. It further lends weight to the argument advanced that OCA hinders the discharge performance of the cell. Deposit, when it was not considered, yielded a value below what was obtained when the plated zinc thickness was accounted for.

The power generated by the discharging cell at a constant current is shown in Figure 9. In a recent report (Bolsted, 1991) of the work done at Johnson Controls (USA), the numbers reported on the power for a stack of Zn/Br<sub>2</sub> battery at 20°C decreased from 0.175 W/cm<sup>2</sup> at 0% DOD to about 0.05 W/cm<sup>2</sup> at 100% DOD. Although all the necessary operating conditions were not given, a comparison (Bolsted, 1991) with Figure 9 shows that using the appropriate data, the present model could be useful in the battery development. The predictions in the figure show that both the organic phase and the thickness of the plated zinc are needed for a good performance prediction. Figure 10 compares the dependence of the energy, and coulombic and voltaic efficiencies on the depth of discharge. Both the energy and voltaic efficiencies decreased very rapidly toward the end of discharge. The coulombic efficiency remained almost constant during the discharge process.

In Figure 11, a comparison is made on the effect of the exponent of Eq. 17. The equation expresses the relationship between the total organic bromine and the total aqueous bromine. As pointed out previously, the exponent and coefficient in Eq. 17 characterize each OCA. It is also assumed commonly that the role of OCA is completely reversible. The equilibrium ratio reported in the literature on OCA is mostly for the charge mode (Eustace, 1980; Kinoshita et al., 1982). However, no one

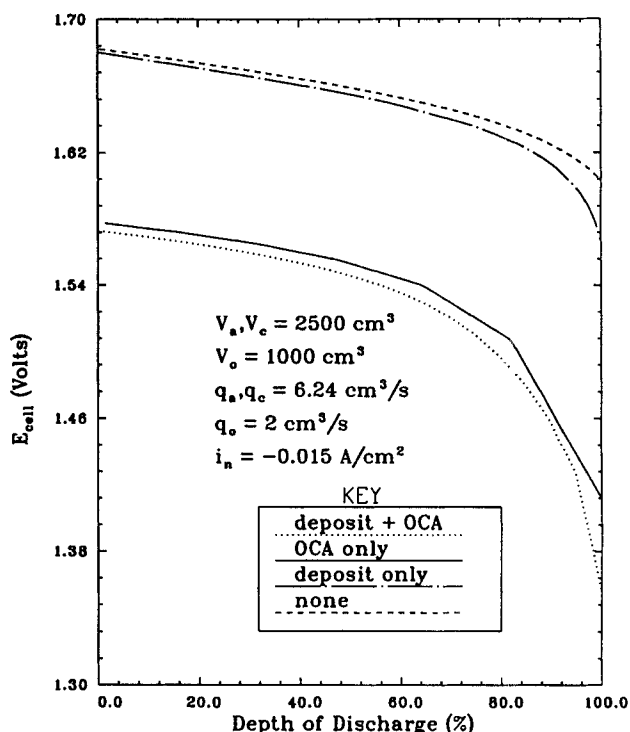


Figure 8. Cell potential during discharge at constant current density.

has attempted (to our knowledge) to study the difference (if any) between the OCA complexation and release mechanism for bromine. The assumption of equilibrium conditions as used here precludes such a study in this work. Figures 11 and 12

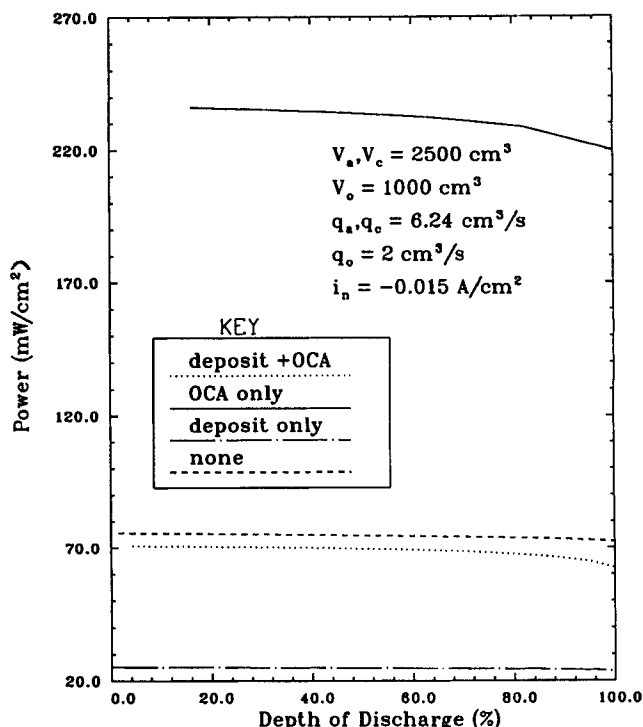


Figure 9. Predicted cell power at a constant current discharge.

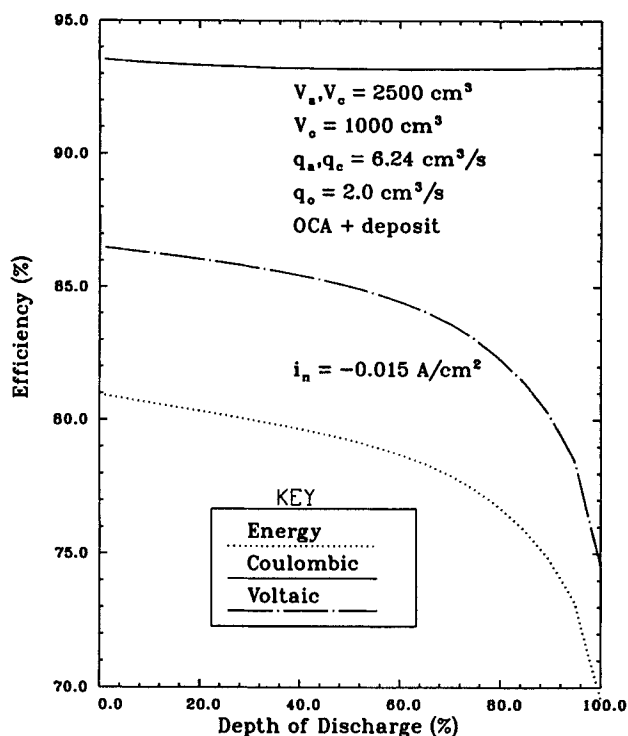


Figure 10. Efficiencies effect on the depth of discharge.

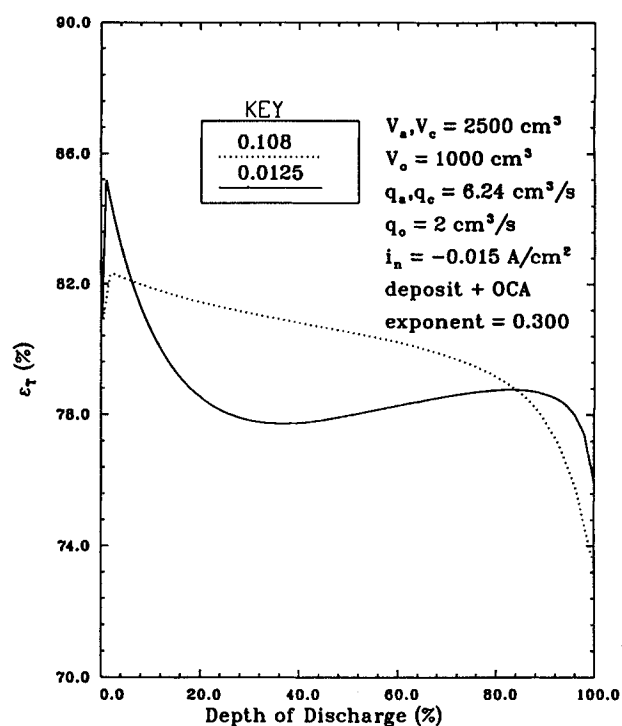


Figure 12. Effect of coefficient of Eq. 17 on predicted cell efficiency during constant current discharge.

compare different organic complexing agents. Figure 11 shows that the better performing organic complexing agents have higher exponents and therefore have better ability at complexing more bromine.

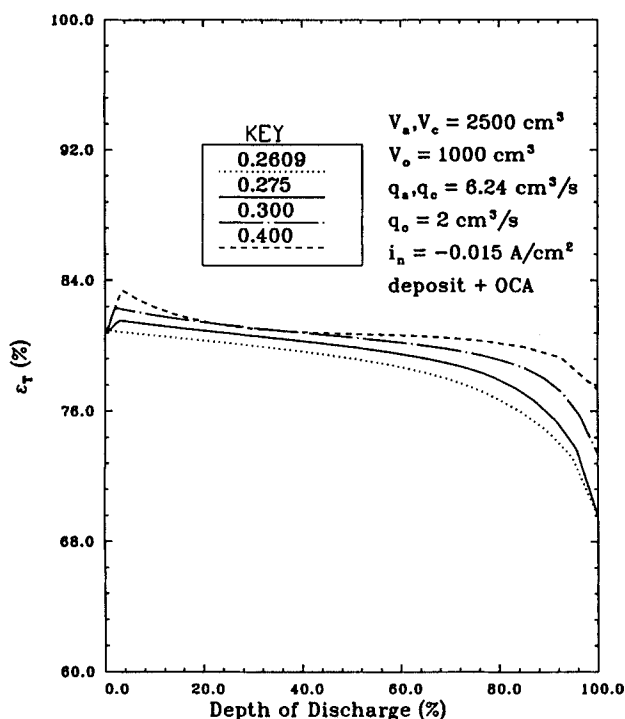


Figure 11. Effect of exponent of Eq. 17 on predicted cell efficiency during constant current discharge.

## Conclusions

A zinc/bromine cell with its associated recirculating systems has been analyzed. The model results show that a consideration of the deposited zinc (during charge) or removed zinc (during discharge) is important in making predictions. Further, the use of organic complexing agent outside the cell has been shown to improve the predicted cell performance during charge. Although the OCA did improve the performance of the cell during discharge, the release of the complexed bromine may degrade cell performance. An equation with a coefficient and an exponent, which relates the total concentration of bromine in the organic phase to the total bromine in the aqueous phase, can be used to characterize an organic complexing agent. The model developed could be useful as a design tool for the Zn/Br<sub>2</sub> flow battery. The model could be extended by the consideration of the Zn/Br<sub>2</sub> flow cell design, in which the organic phase is allowed to circulate through the cell and by modeling the whole cell as a complete time-dependent problem without the quasisteady-state assumption adopted here.

## Acknowledgment

This work was supported by a National Science Foundation Grant No. CBT-8620142.

## Notation

- $c_i$  = concentration of species  $i$ , mol/cm<sup>3</sup>
- $c_i^p$  = fractional change in the concentration of  $i$  over the time period  $t_2 - t_1$
- $c_{i, \text{feed}}$  = feed concentration of species  $i$ , mol/cm<sup>3</sup>
- $c_{i, \text{avg}}$  = outlet concentration of species  $i$  from the electrochemical reactor, mol/cm<sup>3</sup>

$D$  = Equilibrium ratio between the organic and aqueous bromine contents  
 $D_i$  = diffusion coefficient of species  $i$ ,  $\text{cm}^2/\text{s}$   
 $D_{i,e}$  = effective diffusion coefficient of species  $i$  in the separator,  $\text{cm}^2/\text{s}$   
 $D_{i,e,PE}$  = effective diffusion coefficient of species  $i$  in the porous electrode,  $\text{cm}^2/\text{s}$   
 $E_{\text{cell}}$  = applied cell potential ( $U_a - U_c$ ), V  
 $F$  = Faraday's constant, 96,487 C/mol  
 $h$  = channel width, cm  
 $\langle i_{\text{avg}} \rangle$  = average current density during a specified time period, A/cm<sup>2</sup>  
 $i_j$  = current density due to electrochemical reaction  $j$ , A/cm<sup>2</sup>  
 $i_{j,\text{avg}}$  = average current density for species  $j$  in reaction  $k$ , A/cm<sup>2</sup>  
 $i_{o,j,\text{ref}}$  = exchange current density of electrochemical reaction  $j$ , A/cm<sup>2</sup>  
 $K_f$  = equilibrium constant for tribromide reaction,  $\text{cm}^3/\text{mol}$   
 $K_D$  = distribution coefficient between organic and aqueous phases  
 $K_o$  = equilibrium constant in the organic phase,  $\text{cm}^3/\text{mol}$   
 $L$  = electrode length, cm  
 $N_i$  = flux vector of species  $i$ ,  $\text{mol}/\text{cm}^2 \cdot \text{s}$   
 $N_m$  = MacMullin number in the separator  
 $N_{m,PE}$  = MacMullin number in the porous electrode  
 $N_{ni}$  = normal component of the flux of species  $i$ ,  $\text{mol}/\text{cm}^2 \cdot \text{s}$   
 $p$  = pressure drop in the channel,  $\text{g}/\text{cm} \cdot \text{s}^2$   
 $P_{LA}$  = anode side pressure drop per unit length,  $\text{g}/\text{cm}^2 \cdot \text{s}^2$   
 $P_{LC}$  = cathode side pressure drop per unit length,  $\text{g}/\text{cm}^2 \cdot \text{s}^2$   
 $p_{ij}$  = anodic reaction order of species  $i$  in reaction  $j$   
 $q_{ij}$  = cathodic reaction order of species  $i$  in reaction  $j$   
 $q$  = volumetric flow rate through system,  $\text{cm}^3/\text{s}$   
 $q_a$  = volumetric flow of the anolyte,  $\text{cm}^3/\text{s}$   
 $q_c$  = volumetric flow of the catholyte,  $\text{cm}^3/\text{s}$   
 $q_o$  = volumetric flow of the organic phase,  $\text{cm}^3/\text{s}$   
 $R$  = gas law constant, 8.314 J/mol·K  
 $R_i$  = homogeneous production rate of  $i$  in the cell,  $\text{mol}/\text{cm}^3 \cdot \text{s}$   
 $R'_i$  = electrochemical production rate of  $i$ ,  $\text{mol}/\text{cm}^3 \cdot \text{s}$   
 $R_{\text{cstr},i}^*$  = production rate of  $i$  in the circulation tank,  $\text{mol}/\text{cm}^3 \cdot \text{s}$   
 $S_p$  = thickness of the separator, cm  
 $S_{ij}$  = stoichiometric coefficient of species  $i$  in reaction  $j$   
 $t$  = time, s  
 $T$  = temperature, K  
 $U_{j,\text{ref}}$  = open circuit potential of reaction  $j$  based on the reference concentration, V  
 $U_{PE}$  = potential of the porous electrode, V  
 $U_a$  = anode potential, V  
 $U_c$  = cathode potential, V  
 $v$  = electrolyte velocity, cm/s  
 $v_s$  = superficial electrolyte velocity in the separator, cm  
 $v_x$  = flow velocity along the electrode length, cm/s  
 $v_{\text{avg}}$  = average velocity of electrolyte, cm/s  
 $V_{Tr}$  = volume of the recirculating tank,  $\text{cm}^3$   
 $V_{o,Tr}$  = total volume of the organic phase,  $\text{cm}^3$   
 $V_{a,Tr}$  = total volume of the aqueous phase,  $\text{cm}^3$   
 $V_{\text{cell}}$  = electrochemical reactor volume,  $\text{cm}^3$   
 $w$  = electrode width, cm  
 $z_i$  = charge number of species  $i$

## Greek letters

$\alpha$  = aspect ratio,  $S/L$   
 $\alpha_{aj}$  = anodic transfer coefficient for reaction  $j$   
 $\alpha_{cj}$  = cathodic transfer coefficient for reaction  $j$   
 $\beta$  = Darcy's law permeability,  $\text{cm}^2$   
 $\epsilon_i$  = porosity of porous media  $i$   
 $\epsilon_C$  = coulombic efficiency  
 $\epsilon_T$  = total energy efficiency  
 $\epsilon_V$  = voltaic efficiency  
 $\eta_j$  = overpotential at electrode surface, V  
 $\theta_i$  = dimensionless concentration of species  $i$  ( $c_i/c_{i,\text{ref}}$ )  
 $\mu$  = viscosity,  $\text{g}/\text{cm} \cdot \text{s}$

$\rho$  = density of electrolyte,  $\text{g}/\text{cm}^3$   
 $\psi$  = dimensionless number  
 $\tau$  = tortuosity of porous media  
 $\Phi$  = solution potential, V

## Literature Cited

- Bolsted, J., W. Delaney, M. Eskra, R. Vidas, and J. Zagrodnik, "Computer Modeling Studies for Zinc/Bromine Battery Application Design," *Proc. Battery Conf. on Applications and Advances* (1988).  
 Bolsted, J., P. Eidler, R. Miles, R. Petersen, K. Yaccarino, and S. Lott, "Proof-of-Concept Zinc/Bromine Electric Vehicle Battery," Contractor Report SAND91-7029, Sandia National Laboratories, Albuquerque, NM (1991).  
 Chamberlin, J. L., "Status of Zinc/Bromine Batteries," EPRI/LBL Workshop on the Electrochemistry of Zinc/Halogen Batteries, 1, 2 (1983).  
 Chiu, S., and J. R. Selman, "Corrosion of Zinc by Bromine Under Flow Conditions," *AIChE Symp. Ser.*, **254**, 15 (1987).  
 Eustace, D. J., "Bromine Complexation in Zinc-Bromine Circulating Batteries," *J. Electrochem. Soc.*, **127**, 528 (1980).  
 Evans, T. I., and R. E. White, "A Mathematical Model of a Zinc/Bromine Flow Cell," *J. Electrochem. Soc.*, **134**, 866 (1987a).  
 Evans, T. I., and R. E. White, "A Review of Mathematical Modeling of the Zinc/Bromine Flow Cell and Battery," *J. Electrochem. Soc.*, **134**, 2725 (1987b).  
 Hansen, A. G., *Fluid Mechanics*, Wiley, New York (1967).  
 Holland, C. D., and A. Anthony, *Fundamentals of Chemical Reaction Engineering*, Prentice-Hall, Englewood Cliffs, NJ (1979).  
 Kinoshita, K., S. C. Leach, and C. M. Ablow, "Bromine Reduction in a Two-Phase Electrolyte," *J. Electrochem. Soc.*, **129**, 2397 (1982).  
 Lee, J., "Effect of Mass Transfer on the Current Distribution and Dendrite Growth in Electrochemical Reactors," PhD Diss., Illinois Institute of Technology, Chicago (1981).  
 Lee, J., and J. R. Selman, "Effects of Separator and Terminal on the Current Distribution in Parallel-Plate Electrochemical Reactors," *J. Electrochem. Soc.*, **129**, 1670 (1982a).  
 Lee, J., and J. R. Selman, "Zinc Electrodeposition and Dendritic Growth From Zinc Halide Electrolytes," EPRI Report EM-2393, Project 1198-3, Appendix B, Palo Alto, CA (1982b).  
 Mader, M. I., and R. E. White, "A Mathematical Model of a Zn/Br<sub>2</sub> Cell on Charge," *J. Electrochem. Soc.*, **133**, 1297 (1986).  
 Newman, J. S., *Electrochemical Systems*, Prentice Hall, Englewood Cliffs, NJ (1973).  
 Putt, R., "Assessment of Technical and Economic Feasibility of Zn/Br Batteries for Utility Load-leveling," EPRI Report EM-1059, Project 635-1, Appendix M, Palo Alto, CA (1979).  
 Schiesser, W. E., *Differential Systems Simulator*, Version 2 (DSS/2), Release 4, Lehigh University (1988).  
 Selman, J. R., "Performance and Current Distribution Modeling of Batteries and Fuel Cells," *AIChE Symp. Ser.*, **77**, 138 (1981).  
 Simpson, G., and R. E. White, "An Algebraic Model for a Zinc/Bromine Flow Cell," *J. Electrochem. Soc.*, **136**, 2137 (1989).  
 Tomazic, G., "Advances in Zinc Bromine Batteries for Electric Vehicles and Energy Storage at S. E. A.," *Proc. Battery Conf. on Applications and Advances*, R. S. L. Das and H. Frank, eds., Long Beach, CA (Dec., 1989).  
 Van Zee, J. W., R. E. White, P. Grimes, and R. Bellows, "A Simple Model of the Exxon Zinc/Bromine Battery," *Electrochemical Cell Design*, R. E. White, ed., p. 293, Plenum Publishing, New York (1984).  
 Van Zee, J. W., R. E. White, and A. T. Watson, "Simple Models for Diaphragm-type Chlorine/Caustic Cells," *J. Electrochem. Soc.*, **133**, 501 (1986).  
 Van Zee, J. W., "Sodium Hydroxide Production in Diaphragm-Type Electrolyzers," PhD Diss., Texas A&M University (1984).  
 Vanka, S. P., "Second-Order Upwind Differencing in a Recirculating Flow," *AIAA J.*, **25**, 1435 (1987).

Manuscript received Oct. 31, 1990, and revision received June 18, 1991.